

Theoretical calculation of magneto-transport properties in semiconductor devices and comparison to experimental data

Thushari Jayasekera*, Niti Goel, Michael A. Morrison, Kieran Mullen

Department of Physics and Astronomy, The University of Oklahoma, Norman, OK 73019, USA

Available online 19 June 2006

Abstract

Negative bend resistance is a signature of ballistic transport in low-dimension semiconductor devices. We calculate the bend resistance in 4-terminal devices using R-matrix theory. R-matrix theory is a technique first introduced in nuclear physics and recently shown to be a useful tool for calculating transport properties of solid-state devices. We have improved upon the existing implementations of R-matrix theory in device physics by applying a variational basis function approach that dramatically improves the rate of convergence of transmission coefficients. We have also developed a method for calculating transmission coefficients of a device in a nonzero magnetic field. We calculate bend resistance in 4-terminal devices.

© 2006 Elsevier B.V. All rights reserved.

PACS: 75.47.Jn

Keywords: R-matrix theory (RMT); Negative bend resistance (NBR)

1. Introduction

Modern experiments can fabricate ballistic semiconductor devices in which the mean free path of an electron is larger than the size of the device. Transport in these devices has been the focus both in theory and experiment for several years. The transport properties become even more interesting when a magnetic field is applied perpendicular to a two-dimension device. Magneto transport properties of these devices show a number of intriguing properties such as quantum Hall effect, negative bend resistance (NBR). Transport properties of such devices can be studied as a scattering problem via Landauer Büttiker (LB) theory [1]. LB theory uses the transmission coefficients of electrons in the device to calculate transport properties.

We use R-matrix theory (RMT) to calculate the transmission coefficients in the device. RMT was originated to study the nuclear reactions that can be treated in a single spherical-coordinate system. In an earlier paper [2], we have discussed the extension of conventional RMT [3] to nanoscale devices. In this paper, we use RMT to study

the magneto-transport properties of ballistic devices. We calculate the bend resistance of a 4-terminal device and compare our results with experimental data for an InSb device.

2. Bend resistance

NBR is a signature of ballistic transport and has been observed in 4-terminal devices that were lithographically made on semiconductor quantum wells [4]. These devices typically have a 4-terminal square geometry (Fig. 1a) or 4-terminal wedge geometry (Fig. 1b). In this paper we consider only the 4-terminal square geometry. It is not hard to extend our technique to the wedge geometries as we will discuss elsewhere [5].

In the bend resistance experiment [4], (Fig. 1), a current is injected from lead 2 to lead 3 (I_{23}) and the voltage between the leads 1 and 4, V_{14} , is measured. The bend resistance is defined as $R_B = V_{14}/I_{23}$. Goel et al. [4] has reported a NBR at zero magnetic field (Fig. 3) in the 4-terminal InSb devices. If the electron transport is ballistic, charges tend to go forward into lead 4 giving a negative bend resistance. When there is an external

*Corresponding author. Tel.: +1 405 819 8893.

E-mail address: thushari@ou.edu (T. Jayasekera).

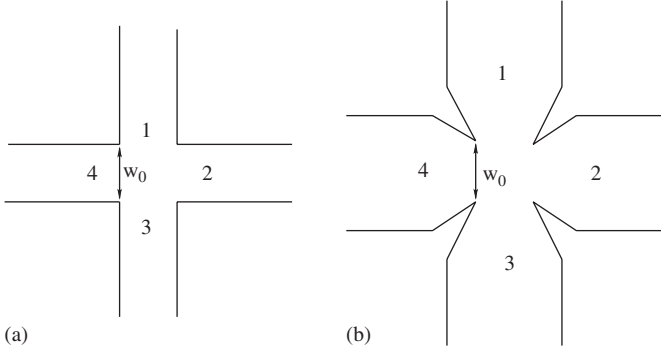


Fig. 1. Schematics of (a) a 4-terminal square junction device and (b) the 4-terminal wedge junction device used in the bend-resistance experiment discussed in the text.

magnetic field, electrons tend to deflect into lead 4 which suppresses the bend resistance.

Since these devices are made of InSb which has a small effective mass ($m^* = 0.0139m_0$, where m_0 is the free electron mass), we must treat the electrons quantum mechanically. We model this experiment using the LB theory, which gives the bend resistance as [6],

$$R_B = \frac{T_{12}T_{32} - T_{42}^2}{(T_{12} + T_{32})[(T_{12} + T_{42})^2 + (T_{32} + T_{42})^2]} \times \frac{h}{2e^2N}, \quad (1)$$

where T_{ij} is the transmission coefficient of electrons from lead j to lead i , h is the Planck's constant, e is the electron charge and N is the number of open subbands at the Fermi energy. Below we explain how to calculate these transmission coefficients using RMT.

3. Two-dimensional RMT in the presence of an applied magnetic field

In a scattering system, typically the asymptotic solutions in the leads are simple while those in the device are less tractable. It would be useful to have a formalism that would allow us to connect the simpler asymptotic solutions to those obtained in the scattering region. RMT allows us to calculate the transmission coefficients in the leads without having to calculate the total scattering wave function of the system [7].

We consider a two-dimensional system with an internal region A that is connected to N external regions or “leads”. We need to solve the time-independent Schrodinger equation for a single electron in the device,

$$\hat{H}|\Psi_{E,n_0}\rangle = E|\Psi_{E,n_0}\rangle, \quad (2)$$

where $|\Psi_{E,n_0}\rangle$ is the scattering state. The subscript E is the scattering energy and n_0 denotes the transverse subband quantum number of the incoming electron. The Hamiltonian \hat{H} is given by

$$\hat{H} = -\frac{\hbar^2}{2m^*}(\mathbf{P} - e\mathbf{A})^2 + V(\mathbf{r}), \quad (3)$$

where \mathbf{A} is the vector potential. We have chosen $V(\mathbf{r}) = 0$ inside the device. The basic idea of the RMT is to divide the system into two parts; an internal scattering region and an external region made of the leads. In the internal region, we expand the scattering state in a basis defined in this region. In each lead of the external region, we expand the scattering state in a basis of transverse eigenfunctions appropriate to that lead. We then use the R-matrix to relate the expansions in the internal and external regions and thus to determine the transmission coefficients in the leads [2].

3.1. Transverse eigenfunctions in the leads

In our current application all leads and the internal region are rectangular. For each lead we define a local coordinate system (x_p, y_p) , where y_p is the transverse coordinate and x_p is the longitudinal coordinate. In the absence of magnetic field, the transverse confining potential in a lead is an infinite square well with $V = 0$. The transverse lead eigenfunctions are therefore simple sine functions. These functions are not applicable if a field is applied, so we seek the transverse functions $f_{p,v_p}(y_p)$ and wave number k_{p,v_p} in the leads, where v_p is the transverse quantum number. We choose the asymmetric gauge for the vector potential, $\mathbf{A} = (-By_p, 0, 0)$. Note that the gauge is different for different regions. It does not matter in the calculation, we only need the eigenfunctions of the Hamiltonian to be a complete set. We measure lengths in terms of a convenient length of the device (which we choose w_0 , the width of the input lead), the energies in terms of $E_0 = \hbar^2/mw_0^2$, and define $\varepsilon = E/E_0$ and $l_B^2 = \hbar/eB$. Since w_0^2/l_B^2 is a measure of the strength of the magnetic field, hereafter we define $B = w_0^2/l_B^2$ [9]. With this notation, the Schrodinger equation in lead p becomes

$$\left[-\frac{1}{2} \frac{d^2}{dy_p^2} + \frac{1}{2} (k_{p,v_p} + y_p B)^2\right] f_{p,v_p}(y_p) = \varepsilon f_{p,v_p}(y_p). \quad (4)$$

We numerically solve for f_{p,v_p} following the theory presented by Tamura and Ando [8], and expand the scattering wave function in lead p as

$$\Psi_{E,n_0}(x_p, y_p) = \sum_{v_p} \tau_{p,v_p}(E) e^{ik_{p,v_p}x_p} f_{p,v_p}(y_p). \quad (5)$$

Once we solve for transmission amplitudes τ_{p,v_p} we can calculate the flux in the p th lead according to,

$$J_p \sim \int dy_p \left[\Psi_{E,n_0}^*(x_p, y_p) \left(-i \frac{d}{dx_p} - A_{x_p} \right) \times \Psi_{E,n_0}(x_p, y_p) + \Psi_{E,n_0}(x_p, y_p) \times \left(i \frac{d}{dx_p} - A_{x_p} \right) \Psi_{E,n_0}^*(x_p, y_p) \right]. \quad (6)$$

Note that the lead eigenfunctions are not orthogonal. One might conclude that this nonorthogonality will result in a position-dependent flux, J_p . This problem does not arise, however, because, two lead eigenfunctions of the

same energy would satisfy [9]

$$\int_{-w_p/2}^{w_p/2} dy f_{p,v_p}(y_p) f_{p,\beta_p}(y_p) (k_{p,v_p} + k_{p,\beta_p} + 2y_p B) = 0. \quad (7)$$

3.2. Bloch eigenfunctions in the interior region

We expand the scattering state $|\Psi_{E,n_0}\rangle$ of Eq. (2) in a basis set defined in the internal region. We cannot expand the state vector in eigenfunctions of \hat{H} , because the operator \hat{H} is not Hermitian in a finite region [10] so its eigenvectors do not form a complete set. We can define a Hermitian operator called the Bloch Hamiltonian [10] as, $\hat{H}_B = \hat{H} + L_0 + L_B$. Here L_0 , the zero-field term is, $L_0 = (\sum_{s_p} \delta(x - s_p) \nabla \cdot \hat{n}_p) / 2$, and the field-dependent term, $L_B = \sum_{s_p} (i\epsilon B) / 2 \times A_p \cdot \mathbf{n}_p$, where \hat{n}_p is the unit vector pointing outwards the p th surface and A_p is the vector potential in the region considered. The summation index s_p runs through all the surfaces and ϵ is positive for upper integration boundaries and negative for lower integration boundaries.

Since \hat{H}_B is Hermitian in the internal region, its eigenfunctions $|\phi_j(x, y)\rangle$ form a complete set. We expand the scattering state in the internal region as, $|\Psi_{E,n_0}\rangle = \sum_j C_j |\phi_j\rangle$, where the ϕ_j 's are calculated using a set of variational basis functions which are not orthogonal inside the interior region. By choosing non-orthogonal basis functions that do not obey a specific boundary condition, we greatly improve the convergence of the R-matrix [2].

3.3. R-matrix formulation

We rearrange Eq. (2) for the state vector

$$(H_B - E)|\Psi_{E,n_0}\rangle = (L_0 + L_B)|\Psi_{E,n_0}\rangle, \quad (8)$$

which gives the expansion coefficients C_j as

$$C_j = \langle \phi_j | \Psi_{E,n_0} \rangle = \frac{1}{H_B - E} \langle \phi_j | (L_0 + L_B) | \Psi_{E,n_0} \rangle. \quad (9)$$

With these coefficients, we can write down the scattering function in the internal region as

$$|\Psi_{E,n_0}\rangle = \sum_j \frac{|\phi_j\rangle}{H_B - E} \langle \phi_j | (L_0 + L_B) | \Psi_{E,n_0} \rangle. \quad (10)$$

We now write Eq. (10) in coordinate space and calculate the result at the openings between the internal region and each lead. We then project the resulting system wave function onto the transverse eigenfunction for each lead. This step defines the scattering function whose asymptotic behavior yields the transmission amplitude τ_{p,v_p} for lead p . From the resulting transmission amplitudes, τ_{p,v_p} , we calculate the transmission coefficients, $T_{ij} = J_i / J_j$, where J_j and J_i are calculated according to Eq. (6).

4. Results and discussion

We consider a device which is made of a sample of InSb with electron concentration $1.90 \times 10^{11} \text{ cm}^{-2}$ which is slightly less than the experimental value. That is because we believe that the electron concentration is decreased during the process of making the device. The Fermi energy at this concentration is 32.7 meV. The width of the symmetric 4-terminal device, w_0 (Fig. 1) is $0.1 \mu\text{m}$ that the Fermi energy, $E_F = 60$ in our energy units, E_0 . Three transverse subbands in each lead are open at the Fermi energy. We calculate the transmission coefficients of electrons in each lead as a function of scattering energy (Fig. 2). At zero magnetic field (Fig. 2a), T_{12} and T_{32} lie on top of one another and T_{42} is always larger than the transmission coefficients for the sidearms. Therefore, more electrons accumulate in the forward lead than in the sidearms giving a negative bend resistance. In the presence of a magnetic field, electrons are more likely to be deflected into sidearms. Thus in (Fig. 2b), we see that at some energies the transmission coefficients, T_{32} is larger than the forward transmission coefficient, T_{42} . In this case fewer electrons accumulate in lead 4, and the NBR is suppressed. The sign and the magnitude of the R_B depend on the ratio of these three transmission coefficients. At different Fermi energies the ratio between various transmission coefficients are different so R_B is very sensitive to the device geometry.

At zero temperature, the transport properties are determined by the electrons at Fermi energy, so we calculate the zero-temperature R_B using Eq. (1). We calculated transmission coefficients for different magnetic fields and calculated the R_B as a function of the magnetic field obtaining results indicated by stars in Fig. 3. The solid curve in this figure is the experimental data of Goel et al [4]

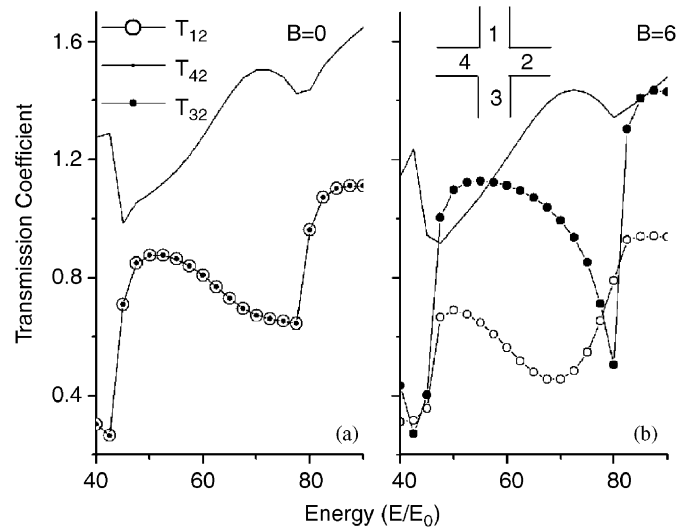


Fig. 2. Transmission coefficients for electrons injected to the 4-terminal square device as shown in the Fig. 1a. Here (a) is the transmission coefficients at zero magnetic field and (b) is the transmission coefficients when $B = w_0^2 / l_B^2 = 6$.

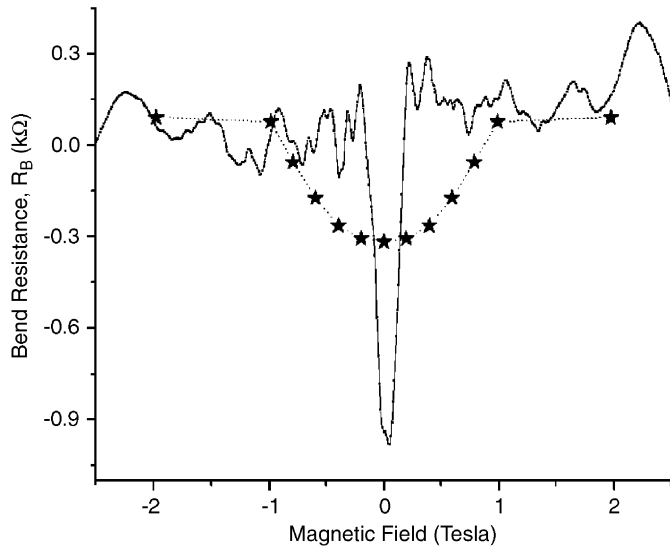


Fig. 3. Bend resistance as a function of the magnetic field, B . Stars are the theoretical values calculated for a device in Fig. 1a with $w_0 = 0.1 \mu\text{m}$ and the solid curve is the experimental observation made by Goel et al. [4] for device sketched in Fig. 1b with $w_0 = 0.5 \mu\text{m}$.

for a device with the geometry shown in (Fig. 1b) with $w_0 = 0.5 \mu\text{m}$. The differences in magnitude in theoretical and experimental results in this figure may arise from

differences between the shape and from the depletion of electrons in the system. Small changes in the electron concentration can change the number of occupied channels.

Acknowledgment

This work is supported by NSF-PHY-0354858, NSF MRSEC DMR-0080054, and NSF EPS-9720651.

References

- [1] M. Büttiker, *Phys. Rev. Lett.* 57 (1986) 1761.
- [2] T. Jayasekera, M.A. Morrison, K. Mullen, unpublished.
- [3] E.P. Wigner, I. Eisenbud, *Phys. Rev.* 72 (1947) 29.
- [4] N. Goel, S.J. Chung, M.B. Santos, K. Suzuki, S. Miyashita, Y. Hirayama, *Physica E* 21 (2004) 761.
- [5] T. Jayasekera, N. Goel, M.A. Morrison, K. Mullen, unpublished.
- [6] Y. Hirayama, T. Saku, S. Tarucha, Y. Horikoshi, *Appl. Phys. Lett.* 58 (1991) 2672.
- [7] R.K. Nesbet, S. Mazevet, M.A. Morrison, *Phys. Rev. A.* 64 (2001) 34702.
- [8] H. Tamura, T. Ando, *Phys. Rev. B* 44 (1991) 1792.
- [9] R.L. Schult, H.W. Wyld, D.G. Ravenhall, *Phys. Rev. B* 41 (1989) 12760.
- [10] C. Bloch, *Nucl. Phys.* 4 (1957) 503.